

# Difference in Peak and Integrated Target Strengths Depending on Signal Duration Using a Time-Domain Physical Diffraction Theory

Keunhwa Lee\*, Sanghyun Park\*, In-Sik Yang\*\*, Won-Tchon Oh\*\*, Woojae Seong\*

\*Dept. of Naval Architecture and Ocean Engineering, Seoul National University, Seoul, KOREA

\*\*Agency for Defense Development, Jinhae, KOREA

(Received September 1 2009; accepted September 5 2009)

## Abstract

The target strength (TS) is calculated from the measured signal using the definition of the peak TS (PTS) or the integrated TS (ITS). These two types of TS sometimes give different results depending on what the pulse duration is. In this paper, we model the scattered time signal by the numerical code based on the physical diffraction theory and examine the effect of the pulse duration on the value of PTS or ITS. The transformed TS (TTS) for the frequency domain is used as a reference solution.

**Keywords:** Target strength, Physical diffraction theory, PTS, ITS

## 1. Introduction

The target strength (TS) is defined as the logarithm of the ratio of the scattered intensity to the incident intensity, while the spreading loss is eliminated [1]. Most of the existing numerical codes [2-4] calculate the TS (the transformed TS, TTS) in the frequency domain on the assumption that the incident wave field is a monochromatic plane wave. However, in the real world, the TS can only be estimated from the time scattered signal with a finite pulse length. Two practical techniques to measure the TS are the peak TS (PTS) and the integrated TS (ITS) [5]. They use either the peak pressure of the incident and scattered pulses or their total integrated energies. Unfortunately, these two TS do not always produce the same result.

In case when long duration incident pulse with a

narrow bandwidth is employed, it is known that the PTS and ITS are equivalent to each other [5]. But, in practice, many researchers would be often faced with the experimental environments where long pulse may not be used, such as acoustic experiments in a small tank. Then, determining the proper pulse duration and estimation technique becomes important in order to provide a consistent and meaningful TS measure.

In this paper, we examine the effects of the incident pulse duration on the calculation of the TS. First, the scattered signals are synthesized with the numerical scattering model based on the physical diffraction theory. From the synthetic signals, two kinds of TS are respectively estimated and compared with the transformed TS.

In Sec. II, we describe the numerical scattering model used in the experiment. The definition of two types of TS is provided in Sec. III. Numerical results are presented and discussed in Sec. IV. Sec. V is a conclusion.

Corresponding author: Keunhwa Lee (nasalkh2@snu.ac.kr)  
Department of Naval Architecture and Ocean Engineering,  
Seoul National University, 151-742, Korea

## II. Numerical Model

A few numerical methods exist for the computation of target scattering [6]. Although the general methods such as finite difference method and boundary element method have been developed, these methods suffer from computational burden that they have the difficulty of modeling the real environment. Therefore, the asymptotic methods are more useful at a limited range of frequency. In this study, we use the numerical model based on the physical theory of diffraction (PTD) [7]. The PTD developed by Ufimtsev is the most advanced asymptotic method, remedying singularities of the classical ray method.

Asymptotically, at mid-high frequency range, the scattered field  $p_s$  is divided into two physical terms as follows:

$$p_s = p_{ray} + p_{diff} \quad (1)$$

where  $p_{ray}$  and  $p_{diff}$  represent the reflected ray and the diffraction part.

Direct calculation of Eq. (1) is not easy, since the reflected ray may have singularities such as caustics and diffraction components that are given by complex integral or infinite asymptotic series.

These difficulties were first solved by Ufimtsev. He removed the singularity of the ray through the integral approach with the Kirchhoff assumption where the complexity of the diffraction component was simplified using *the method of canonical problems* for a wedge.

By Ufimtsev's idea, Eq. (1) is rewritten as

$$p_s = (p_{ray} + p_{K\_diff}) + (p_{diff} - p_{K\_diff}) = p_{Kirchhoff} + p_{PTD\_diff} \quad (2)$$

where  $p_{K\_diff}$  represents the diffraction term of Kirchhoff integral,  $p_{Kirchhoff} = (p_{ray} + p_{K\_diff})$  and  $p_{PTD\_diff} = (p_{diff} - p_{K\_diff})$ .

When the incident spherical wave impinges on the impedance polygon within the unbounded acoustic

medium as shown in Fig. 1, we derive the following formulae for two final terms of Eq. (2).

$$p_{Kirchhoff}(\vec{r} | \vec{r}_0) = \frac{e^{jk_0(R_n + R_s)}}{(4\pi)^2 R_s R_R} \frac{[(\vec{R}_n + \vec{\zeta}) + \tilde{R}(\omega)(\vec{R}_n - \vec{\zeta})] \cdot \vec{\eta}}{W^2} \quad (3)$$

$$\sum_{i=1}^n (\vec{w} \cdot \vec{b}_i) \text{sinc}(k_0 \frac{\vec{w} \cdot \vec{b}_i}{2}) e^{jk_0 \frac{w}{2} (\vec{a}_i \cdot \vec{a}_i)}$$

where  $\tilde{R}(\omega)$  is plane wave reflection coefficient,  $n$  is total number of vertices of the polygon facet,  $\vec{R}_R$  is vector drawn from the origin of a facet to field point,  $\vec{R}_s$  is vector drawn from source point to the origin of a facet,  $\vec{R}_n = \vec{R}_R / |\vec{R}_R|$  is unit vector drawn from the origin of a facet to field point,  $\vec{\zeta} = \vec{R}_s / |\vec{R}_s|$  is unit vector drawn from source point to the origin of a facet,  $\vec{\eta}$  is unit normal vector to the facet,  $\vec{w} = \vec{\zeta} - \vec{R}_n$ ,  $\vec{w}^* = \vec{w} \times \vec{\eta}$ ,  $W$  is the length of the projection  $\vec{w}$  onto the facet,  $\vec{a}_i$  is the vector from the origin of a facet to  $i$ th vertex, and  $\vec{b}_i = \vec{a}_{i+1} - \vec{a}_i$  with  $\vec{a}_{n+1} = \vec{a}_1$ .

$$p_{PTD\_diff}(\vec{r} | \vec{r}_0) = \frac{1}{(4\pi)^2} \sum_{i=1}^l |\vec{b}_i| [(1 + \tilde{R}(\omega)) F_i^{(1)} - (1 - \tilde{R}(\omega)) F_i^{(2)}] \text{sinc}(k_0 \frac{\vec{w} \cdot \vec{b}_i}{2}) \frac{e^{jk_0(R_{sd_i} + R_{rd_i})}}{R_{sd_i} R_{rd_i}} \quad (4)$$

where  $R_{sd_i}$  is the distance between source point and the center of the  $i$ -th edge,  $R_{rd_i}$  is the distance between

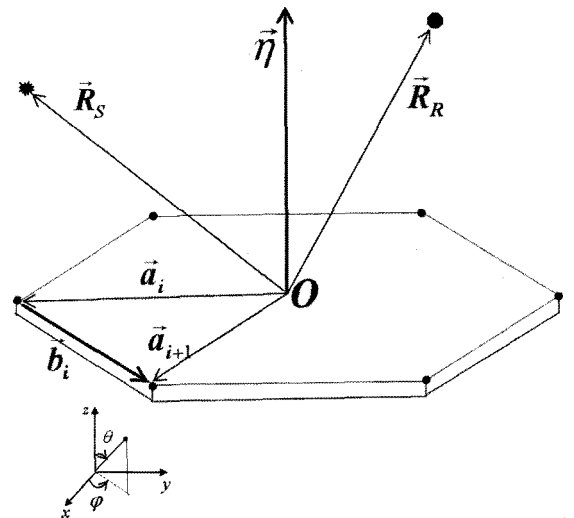


Fig. 1. Definition of the vectors for a polygon target.

field point and the center of the  $i$ -th edge, and  $F_i^{(0)}$  and  $F_i^{(1)}$  are the 3D diffraction coefficients of Ufimtsev.

The precise derivation of Eq. (3) is referred to the works of Gordon [8] and Lee and Seong [9]. The details of Eq. (4) will be presented in a future paper.

Thus, if an arbitrary 3D target is divided into polygons, the target scattering field can be calculated using Eqs. (2)–(4). Then, the scattered time signal can be transformed from the target scattering field using Fourier transform as follows.

$$P_s(t) = \frac{1}{2\pi} \int_{-\infty}^{\infty} s(\omega) P_s(\omega) e^{-j\omega t} d\omega, \quad (5)$$

where  $s(\omega)$  is a source function.

### III. Three Kinds of Target Strength Definition

When obtaining TS from the measured signal, two kinds of definitions are widely used. One is PTS defined as the ratio between the peak scattered signal and the peak incident signal as follows [5].

$$TS_p = 10 \log_{10} \left( \max[P_s^2(t)] / \max[P_i^2(t)] \right). \quad (6)$$

Another is ITS defined as the ratio between the time integrated scattered and incident signal as follows.

$$TS_i = 10 \log_{10} \left( \int_0^{\tau} P_s^2(t) dt / \int_0^{\tau} P_i^2(t) dt \right). \quad (7)$$

Here,  $\tau$  is the pulse length.

Besides above two definitions, the other TS frequently employed is the transformed TS defined as,

$$TS_t = 10 \log_{10} \left( p_s^2(\omega) / p_i^2(\omega) \right). \quad (8)$$

We note that Eqs. (7) and (8) mathematically should show same results for an ideal case, such as the incident source with a narrow bandwidth.

## IV. Results and Discussion

We use an example to illustrate how the PTS and ITS depend on the signal pulse duration employed. In the illustrative example, a rectangular steel plate of  $0.2 \text{ m} \times 0.2 \text{ m}$  is used as the target to simulate the scattered signal. The distance of the mono-static sonar and the target is 3 m. The sinusoidal pulse is chosen as the source pulse. The center frequency of the pulse is 134 kHz and two durations of 5 (short) and 100 (long) cycles are employed. The water sound speed is 1500 m/s and no absorption is considered.

For the modeling, the rectangular target is divided into 12 sub-surfaces to consider the near-field effect. The numerical calculation is performed by Eqs. (2)–(5) with 4096 time samples and the sampling frequency of 1.34 MHz.

Fig. 2 and Fig. 3 show the normalized scattered signals for the pulse durations of 5 and 100 cycles. The mono-static sonar moves along the elevation angle from the x-axis when the edges of target plate are set parallel to x and y axis, respectively. As shown in Fig. 2, there occur two highlight points at two edges parallel to the y-axis.

For these figures, we can confirm two natural characteristics of the target scattered signal. First, the pulse length of the scattered signal changes as the distances between the sonar and the target edges vary due to

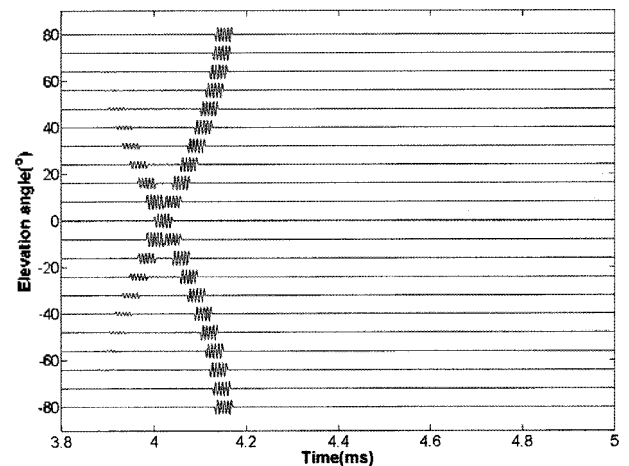


Fig. 2. The normalized scattered time signal for the elevation angle with the incident pulse duration of 5 cycles.

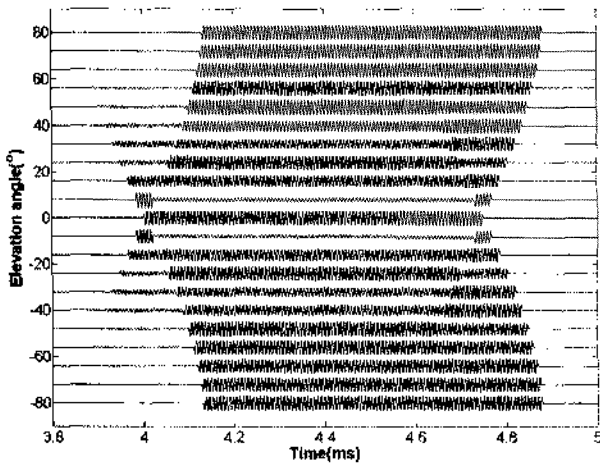


Fig. 3. The normalized scattered time signal for the elevation angle with the incident pulse duration of 100 cycles.

different source location. Second, if the incident pulse duration is short, the total signals from each highlight points do not exhibit 'steady state'.

In Fig. 4, we compare the transformed and peak TS for the pulse duration of 5 and 100 cycles. Near the main lobe (maximum target strength), two results for 5 and 100 cycles show very similar pattern. This is because the time difference between highlight points is very small near the main lobe so that the scattered signals rapidly reach the *steady state* condition. However, as the time difference becomes larger away from the main lobe, the result for 5 cycles shows more deviation from the transformed TS. The result for 100 cycles seems to be similar to the transformed TS for most of elevation angles with a slight deviation observed for few angles. This is because the peak point of the scattered signal occasionally appears in the instantaneous interval of time signal, not the steady state interval as shown in Figs. 1 and 2. A method to solve this problem is to eliminate the instantaneous interval by the time-windowing before picking up the peak point.

In Fig. 5, we plot the results for the integrated TS. Similar to the peak TS case, the result for 5 cycles match the transformed TS only near the main lobe. The result for 100 cycles is equal to the transformed TS in all elevation angles and more accurate than the peak TS of 100 cycles in Fig. 4. This is easily explained by Parseval's theorem for narrowband signal.

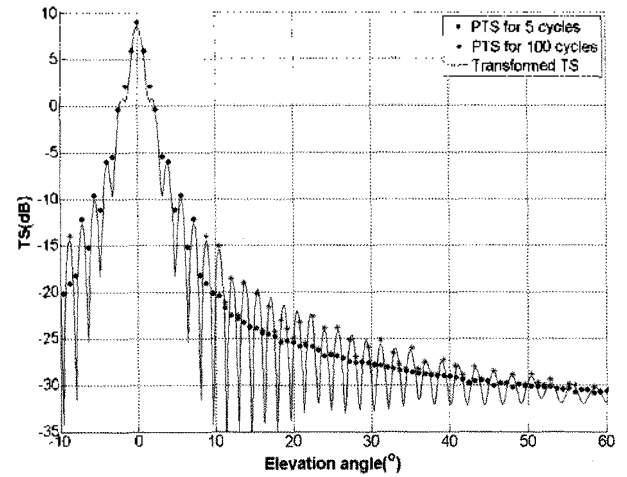


Fig. 4. Comparison of the peak TS and the transformed TS.

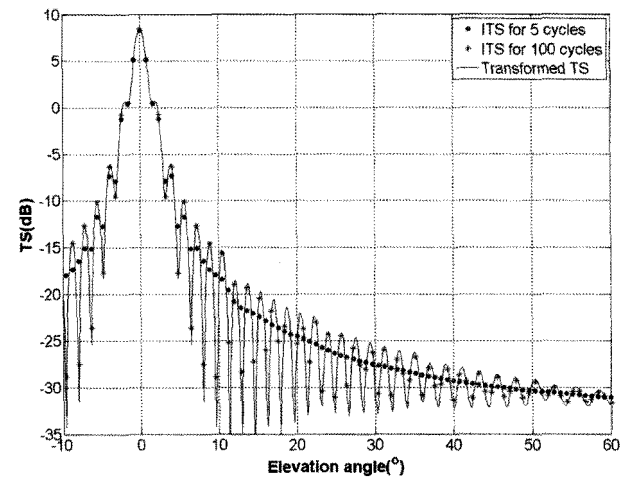


Fig. 5. Comparison of the integrated TS and the transformed TS.

## V. Conclusion

In order to examine the effect of the incident pulse length on the calculation of the TS, we model the scattered time signal by the numerical tool based on the PTD and estimate the TS by the two methods (the peak and integrated TS).

For the scattered signal of the *non-steady state*, both the peak and integrated TS do not match the transformed TS. This is because non-steady signal does not exhibit all interference patterns from every highlight points. That means the PTS of non-steady scattered signal does not necessarily equal the total TS of the global target but a part of it.

When the incident pulse duration is sufficiently long

such that the scattered signal becomes steady, the peak and integrated TS show coincidence with the transformed TS. In our example, the integrated TS gave better result than the peak TS. Degeneration of the peak TS occurs when the peak of instantaneous interval is larger than that of steady state interval, such as the destructive interference among highlight points. This difficulty may be solved by applying time-windowing before picking up the peak.

Although we only studied the effect of pulse length in this paper, the SNR (signal to noise ration), pulse type, and pulse bandwidth are important parameters affecting the performance of the TS estimation. More general analysis will be required as future works.

---

## References

---

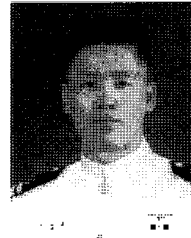
1. R. J. Urick, *Principles of underwater sound*, McGraw-Hill Book, 1983.
2. K. Lee, W. Seong, and Yongtaek Joo, "Modeling of scattering from targets in an oceanic waveguide using Kirchhoff/diffraction method," *J. Acous. Soc. of Am.*, vol. 124, pp. 3757, 2008.
3. Y. Choi, K. Shin, J. You, J. Kim, W. Joo, Y. Kim, J. Park, S. Choi, and W. Kim, "Numerical modeling and experimental verification for target strength of submerged objects," *J. Korean Soc. of Ocean Engineers*, vol. 19, pp. 64-70, 2005.
4. K. Kim, D. Cho and W. Seong, "Simulation of time-domain acoustic wave signals backscattered from underwater targets," *J. Acous. Soc. Kr.*, vol. 27, no. 3, pp. 140-148, 2008.
5. A. D. Waite, *Sonar for practising engineers*, John Wiley & Sons, Ltd., West sussex, 2002.
6. C. Jenn, *Radar and laser cross section engineering*, AIAA Inc., Washington, DC, 1995.
7. P. Ulimtsev, *Fundamentals of the physical theory of diffraction*, Wiley-IEEE press, New Jersey, 2007.
8. W. B. Gordon, "Far field approximation to the Kirchhoff-Helmholtz representations of scattered fields," *IEEE Transactions on antennas and propagation*, AP-23, pp. 590-592, 1975.
9. K. Lee and W. Seong, "Time-domain Kirchhoff model for acoustic scattering from an impedance polygon facet," *J. Acous. Soc. Am.*, vol. 126, pp. EL14-EL21, 2009.

## 【Profile】

• Keunhwa Lee

The Journal of the Acoustical Society of Korea, vol. 27, no. 3, 2008.

• Sanghyun Park



2000. 3: Dept. of management science, Naval Academic, Korea (B.S.)  
 2005. 3: Dept. of earth and marine science, Hanyang Univ., Korea (M.S.)  
 2008. 3-present: Doctoral candidate in the dept. of ocean eng., Seoul Nat'l Univ., Korea

• In-Sik Yang

The Journal of the Acoustical Society of Korea, vol. 23, no. 2, 2004.

• Won-Tchon Oh

The Journal of the Acoustical Society of Korea, vol. 20, no. 2, 2001.

• Woojae Seong

The Journal of the Acoustical Society of Korea, vol. 27, no. 3, 2008.